



Gut microbiota dysbiosis-induced activation of the intrarenal renin-angiotensin system is involved in kidney injuries in rat diabetic nephropathy

Journal:	<i>Acta Pharmacologica Sinica</i>
Manuscript ID	APS-17892.R3
Manuscript Type:	Article
Date Submitted by the Author:	23-Oct-2019
Complete List of Authors:	Lu, Chen Chen Hu, Ze Bo Wang, Ru Hong, Ze Hui Lu, Jian Chen, Pei Pei Zhang, Jia Xiu Li, Xue Qi Yuan, Ben Yin Huang, Si Jia Ruan, Xiong Zhong LIU, Bi-cheng; Institute of Nephrology, Zhongda Hospital, Southeast University School of Medicine Ma, Kun Ling
Keywords:	Gut microbiota, Diabetic nephropathy, renin-angiotensin system, plasma acetate, broad-spectrum antibiotics
Subject Area:	Endocrine Pharmacology

SCHOLARONE™
Manuscripts

1
2
3 **1 Gut microbiota dysbiosis-induced activation of the intrarenal renin-angiotensin**
4
5 **2 system is involved in kidney injuries in rat diabetic nephropathy**
6
7
8

9 3 Chen Chen Lu¹, Ze Bo Hu¹, Ru Wang², Ze Hui Hong³, Jian Lu¹, Pei Pei Chen¹, Jia
10
11 4 Xiu Zhang¹, Xue Qi Li¹, Ben Yin Yuan¹, Si Jia Huang¹, Xiong Zhong Ruan⁴, Bi
12
13 5 Cheng Liu¹, Kun Ling Ma^{1,*}
14
15
16

17 6 1 Institute of Nephrology, Zhong Da Hospital, School of Medicine, Southeast
18
19 7 University, Nanjing, 210009, China.
20
21

22 8 2 Institute of Life Science, Southeast University, Nang Jing,
23
24 9 China.
25
26

27 10 3 Department of Genetics and Developmental Biology, Southeast University School of
28
29 11 Medicine, Nang Jing City, China.
30
31

32 12 4 Centre for Nephrology, University College London (UCL) Medical School, Royal
33
34 13 Free Campus, UK.
35
36

37 14 * **Correspondence to:**
38
39

40
41
42 15 Kun Ling Ma, Email : klma05@163.com
43
44

45 16 **Running Head:** Gut micorbiota and diabetic nephropathy
46
47

48 17
49

50 18
51
52
53
54
55
56
57
58
59
60

1
2
3
4
5 20 **Abstract**
6
7

8 21 Some studies have shown that gut microbiota along with its metabolites is closely
9
10 22 associated with diabetic mellitus (DM). In this study we explored the relationship
11
12 23 between gut microbiota and kidney injuries of early diabetic nephropathy (DN) and its
13
14 24 underlying mechanisms. Male SD rats were intraperitoneally injected with
15
16 25 streptozotocin to induce DM. DM rats were orally administered compound
17
18 26 broad-spectrum antibiotics for 8 weeks. After the rats were sacrificed, their blood,
19
20 27 urine, feces and renal tissues were harvested for analyses. We found that compared
21
22 28 with the control rats, DM rats had abnormal intestinal microflora, increased plasma
23
24 29 acetate levels, increased proteinuria, thickened glomerular basement membrane, and
25
26 30 podocyte foot process effacement in the kidneys. Furthermore, the protein levels of
27
28 31 angiotensin II, angiotensin-converting enzyme, and angiotensin II type 1 receptor in
29
30 32 the kidneys of DM rats were significantly increased. Administration of
31
32 33 broad-spectrum antibiotics in DM rats not only completely killed most intestinal
33
34 34 microflora, but also significantly lowered the plasma acetate levels, inhibited
35
36 35 intrarenal RAS activation, and attenuated kidney damage. Finally, we showed that
37
38 36 plasma acetate levels were positively correlated with intrarenal angiotensin II protein
39
40 37 expression ($r=0.969$, $P<0.001$). In conclusion, excessive acetate produced by
41
42 38 disturbed gut microbiota might be involved in the kidney injuries of early DN through
43
44 39 activating intrarenal RAS.
45
46
47
48
49
50

51
52 40 **Keywords:** diabetic nephropathy; gut microbiota; plasma acetate; renin-angiotensin
53
54 41 system; broad-spectrum antibiotics
55
56
57
58
59 42
60

44 Introduction

45 As a chronic microvascular complication of diabetes, DN has become one of the
46 major causes leading to the death of diabetic patients. According to the 8th IDF
47 Diabetes Atlas, 425 million adults were diagnosed with diabetes worldwide in 2017,
48 and this population has been expected to grow by 48% by 2045 [1]. The rapid growth
49 of diabetes has led to a dramatically increasing prevalence of DN. In China, due to the
50 rapid development of the social economy and lifestyle changes, the prevalence of
51 diabetes is also on the rise. According to the latest survey data in China, the
52 prevalence of diabetes in adults is 11.6%, and the total number of diabetic patients is
53 as high as 114 million, nearly half of which also have DN [2]. However, due to the
54 limited diagnosis of early DN, most of the newly diagnosed patients have already
55 progressed to stage III or IV, which is basically irreversible. Therefore, it is of great
56 importance to clarify the pathophysiological changes in the early stages of DN and
57 formulate intervention strategies for clinical diagnosis and treatment.

58 The activation of the intrarenal renin angiotensin system (RAS) has long been
59 considered one of the initiators of DN. It has been reported that under diabetic
60 conditions, the circulating RAS is normal or decreased, while local RAS is highly
61 activated in the kidney. In addition, renal tissue is sensitive to angiotensin II (Ang II),
62 leading to renal vasoconstriction, higher resistance of the glomerular efferent artery,
63 and increased sodium and water reabsorption, all resulting in increased blood pressure
64 and glomerular hypertension [3]. In addition, Ang II can also promote the phenotypic

1
2
3
4 65 transformation of glomerular endothelial cells and podocytes, the deposition of
5
6 66 extracellular matrix, and the secretion of inflammatory and profibrotic chemokines
7
8
9 67 and factors, accelerating the progression of DN [4, [5, [6, [7].
10

11
12
13 68 In recent years, the effect of gut microbiota on diabetes and its complications has
14
15 69 aroused great interest. The gut microbiota of humans weighs approximately 1.5 to 2.0
16
17
18 70 kg, including approximately 100 trillion bacteria, the distribution density of which
19
20
21 71 increases gradually from the proximal end to the distal intestine. The composition of
22
23 72 gut microbiota in the host is associated with several factors, such as genetic and
24
25
26 73 environmental influence and long-term dietary patterns, and this microbial
27
28
29 74 community usually manifests as a state of equilibrium between different groups in the
30
31 75 gut. While the host provides nutrients to the gut microbiota, the latter helps digest
32
33
34 76 complex carbohydrates, producing immune molecules, short-chain fatty acids (SCFAs)
35
36
37 77 and other metabolites that exert immune and metabolic functions [8, [9]. Studies have
38
39 78 revealed notable differences in the gut microbiota between diabetic and healthy
40
41
42 79 people [10]. In the intestines of healthy people, there are rich butyrate-producing
43
44
45 80 bacteria, such as *Escherichia coli*, *Clostridium*, etc. In patients with type 2 diabetes
46
47
48 81 (T2DM), butyrate-producing bacteria are significantly reduced compared with
49
50
51 82 increasing opportunistic pathogens [11]. Karlsson *et al* [12] have shown that
52
53
54 83 postmenopausal women with T2DM in Europe have significant insulin resistance,
55
56
57 84 partly because of a significant decrease in the abundance of *Faecalibacterium*
58
59
60 85 *prausnitzii* and *Roseburia*, which are known as dwellers and butyrate producers of the
86 human gut [13] and have been linked to improved insulin sensitivity and diabetes [14,

1
2
3
4 87 [15]. Larsen *et al* [16] found that the abundance of intestinal *Firmicutes* in adult male
5
6 88 patients with T2DM decreased significantly, while the abundance of *Bacteroides* and
7
8
9 89 *Proteobacteria* increased, and the ratio of *Bacteroides/Firmicutes* was correlated with
10
11 90 patients' glucose tolerance and blood glucose levels. Compared with healthy controls,
12
13 91 the abundance of *Firmicutes* increased in T1DM patients, while the abundance of
14
15 92 *Bacteroidetes* decreased [17, [18]. In animal studies, treatment with a prebiotic
16
17 93 (oligofructose) in high-fat-fed diabetic mice not only increased the bifidobacterial
18
19 94 content of their guts but improved their glucose tolerance and insulin resistance as
20
21 95 well [19]. Therefore, the gut microbiota might be closely related to the occurrence and
22
23 96 development of diabetes.

24
25
26
27
28
29
30
31 97 Recent studies have found that under the stimulation of injurious factors, the gut
32
33 98 microbiota could produce excessive SCFAs such as acetate, mediate immune
34
35 99 disorders and chronic inflammatory reactions of the host, and promote the occurrence
36
37 100 of diseases such as diabetes, obesity, and inflammatory bowel disease [20, [21, [22].
38
39 101 The gut microbiota of high-fat-fed rats has been reported to promote insulin secretion
40
41 102 and aggravate insulin resistance by synthesizing large amounts of acetate [23].
42
43
44
45
46
47

48 103 Studies have shown that SCFAs are involved in physiological pathways by binding to
49
50 104 their receptors, G protein-coupled receptors (GPCRs) and olfactory receptors (OlfR).
51
52 105 Reportedly, functional receptors of SCFAs include GPR43, GPR41, GPR109, OlfR78
53
54 106 [22, [24] and so on. Brown *et al* [25] found that the smooth muscle cells of renal
55
56 107 arteries express SCFA receptors, and among them, GPR41 and OlfR78 are relatively
57
58
59
60

1
2
3
4 108 abundant. Intestinal-derived propionic acid can bind to the renal arteriolar Olfr78 and
5
6 109 activate intrarenal RAS, further increasing the secretion of renin and angiotensin and
7
8
9 110 thus regulating circulating and glomerular pressure.
10

11
12
13 111 Therefore, we speculated that in the development of diabetes, the gut microbiota was
14
15 112 likely to produce excessive SCFAs, especially acetate, which could bind to
16
17
18 113 renal-related signal receptors, thus activating intrarenal RAS and mediating the early
19
20
21 114 pathophysiological processes of DN.
22

23 24 115 **Methods**

25 26 27 28 116 *Experimental animals and measurement of general parameters*

29
30
31
32 117 Eight-week-old healthy male Sprague-Dawley rats were kept under the following
33
34 118 conditions: a constant 12-hour photoperiod, temperature of 21-23°C, and free access
35
36
37 119 to food and water. After 2 weeks of adaptive feeding, these SD rats were randomly
38
39
40 120 divided into three groups: the control group, diabetic (DM) group, and diabetic rats
41
42 121 treated with antibiotics (DM+AB) (n=10). The latter two groups were
43
44
45 122 intraperitoneally injected with streptozotocin at a dose of 65.0 mg/kg (Sigma, USA),
46
47
48 123 and blood glucose levels were measured 3 days after the injection to confirm the
49
50
51 124 establishment of diabetic models. All rats of the three groups were normally fed,
52
53 125 while the DM+AB group were orally given compound antibiotic solution, consisting
54
55 126 of 1 g/L ampicillin, 1 g/L neomycin, 0.5 g/L vancomycin and 0.1 g/L amphotericin B.
56
57
58 127 All rats were sacrificed after 8 weeks, with blood, urine, feces and renal tissues
59
60

1
2
3
4 128 harvested (kidney weights were measured at the time of sacrifice). The concentrations
5
6 129 of blood glucose (BG) were determined by a blood-glucose meter (Shanghai Johnson
7
8
9 130 & Johnson Medical Devices Company). Serum creatinine (Scr) and blood urea
10
11 131 nitrogen (BUN) were measured by an automatic analyzer (Hitachi Tokyo, Japan). The
12
13
14 132 rats were kept alone in metabolic cages to collect their 24-hour urine samples, of
15
16
17 133 which the level of 24-hour urinary protein was quantitatively analyzed by the Lowry
18
19 134 assay. The measurement of blood pressure in the three groups was performed at the
20
21
22 135 Animal Core Facility of Nanjing Medical University.

23
24
25
26 136 The procedures for the animal experiments were approved by the Ethical Committee
27
28 137 of Southeast University and followed the latest version of the Declaration of Helsinki.

29
30
31
32 138 ***Morphological analysis***

33
34
35
36 139 After the kidneys were removed, the tissues were decapsulated and fixed in 4%
37
38 140 paraformaldehyde and glutaraldehyde. After 48 hours, fixed tissues were embedded in
39
40
41 141 paraffin for observation of the pathological changes under light microscopy (Olympus,
42
43
44 142 Japan) or embedded in 1% lanthanum nitrate for ultramicrostructural observation of
45
46 143 the podocytes and glomerular basement membrane (GBM) under electron microscopy
47
48
49 144 (JEM-1010, Japan). The tissues were cut into 2- μ m-thick slices and then stained with
50
51
52 145 periodic acid-Schiff (PAS) solution and wheat germ agglutinin (WGA) after removing
53
54 146 the paraffin. Immunofluorescent staining of the tissue slices was performed using
55
56
57 147 primary antibodies against Wilms' tumor 1 (WT-1) and nephrin (Santa Cruz, USA)
58
59 148 and examined by laser confocal microscopy (Leica, Germany).

1
2
3
4 149 ***Measurement of plasma acetate***
5
6
7

8 150 The levels of plasma acetate were measured by gas chromatography. Briefly, 200
9
10 151 mmol/L 4-methylvaleric acid (Macklin, China) was used as an internal standard stock
11
12 152 solution, while 1000 mmol/L acetic acid (Sigma-Aldrich, USA) was used as the
13
14 153 acetate standard stock solution. The diluent and extracting solvent were ethyl acetate.
15
16 154 Different concentrations of acetate standards were prepared with 18 mmol/L internal
17
18 155 standard. A total of 50 μ l of plasma was spiked with 90 μ l of 200 mmol/L stock
19
20 156 solution of internal standard and acidified with 10 μ l of hydrochloric acid. After
21
22 157 shaking for 30 seconds, the mixture was sonicated for 1 minute and placed at 4°C
23
24 158 until layering. After centrifugation for 5 minutes at a speed of 12,500 rpm, the organic
25
26 159 phase was filtrated using a 0.22- μ m filter. A 1- μ l injection of standards and filtrated
27
28 160 samples was used for gas chromatography analysis with a DB-23 column (30
29
30 161 m*0.250 mm, Agilent, USA) at a speed of 1 ml/min. The split ratio was 7:1. The
31
32 162 carrier gas was nitrogen. The initial temperature was 90°C, which increased to 150°C
33
34 163 (15°C/min). It was then heated to 170°C (5°C/min), gradually increasing to 250°C
35
36 164 and waiting for 2 minutes. The standard curve was made according to the
37
38 165 concentration and peak area of acetate standards to that of the internal standard. The
39
40 166 plasma acetate concentration was then quantified.
41
42
43
44
45
46
47
48
49
50
51
52

53 167 ***16S ribosomal DNA sequencing analysis***
54
55
56

57 168 The gene sequencing of gut microbiota was performed using 16S ribosomal DNA
58
59 169 (rDNA) sequencing technology. Fresh fecal specimens were collected using sterile
60

1
2
3
4 170 tweezers and tubes and stored at -80°C. The total DNA of the fecal bacteria was
5
6
7 171 extracted according to the manual of the QIAamp DNA Stool Mini kit (QIAGEN,
8
9 172 Hilden, Germany). Briefly, feces were homogenized and lysed in ASL buffer. The
10
11
12 173 mixture was centrifuged at 14,000 rpm for 1 minute. An InhibitEX tablet was
13
14 174 dissolved in the supernatant, followed by centrifugation. Proteinase K and ethanol
15
16
17 175 were added to the supernatant. Lysates were then loaded onto the QIAamp spin
18
19
20 176 column with a QIAamp membrane. The column was efficiently washed in two steps
21
22
23 177 with repeated centrifugation. Lastly, purified DNA was eluted in low-salt buffer. PCR
24
25 178 amplification of the variable region 4-5 of bacterial 16S rDNA was conducted through
26
27
28 179 double 8 cycles to yield detectable products. The amplicons were mixed and purified
29
30
31 180 to construct the gene library after quantification by real-time PCR. Sequencing was
32
33
34 181 performed on the Illumina MiSeq2×300bp platform. Operational taxonomic unit
35
36
37 182 (OTU) picking (97% nucleotide sequence identity) was assigned using the ribosomal
38
39
40 183 database project (RDP) classifier. Chimeric sequences were removed using UCHIME.
41
42
43 184 The alpha diversity analysis was performed with mothur (Version 1.33.3), while the
44
45
46 185 beta diversity analysis was performed with R program (Version 3.2.3).

47 186 ***Measurement of circulating RAS***

48
49
50 187 The levels of renin, Ang I and Ang II in the plasma of the three groups were measured
51
52
53 188 by a radioimmunoassay kit (Beijing North Institute of Biological Technology, China)
54
55
56 189 in accordance with the instructions. The method for determining the level of plasma
57
58
59 190 renin activity (PRA) is as previously described [26]: The optimal dose of trypsin
60

1
2
3
4 191 (Invitrogen, USA) added was confirmed by constructing a dose-response curve, which
5
6 192 was used for subsequent determination. Plasma samples were treated with trypsin and
7
8
9 193 kept at 4°C, pH 7.3, for 30 minutes for activation, after which trypsin inhibitor was
10
11 194 added for 15 minutes at room temperature to terminate the activation. The levels of
12
13 195 renin activation before and after the addition of trypsin were measured, and the PRA
14
15 196 level of each sample was the total renin level by trypsin activation minus the renin
16
17 197 level before trypsin addition.
18
19
20
21
22

23 198 *Western blot analysis*

24
25
26
27 199 Proteins were extracted from kidney tissues, and the protein concentration of each
28
29 200 sample was measured. By adding lysate, loading buffer, and ddH₂O, the protein
30
31 201 concentration and volume of each sample were equal, and all samples were boiled at
32
33 202 100°C for 10 minutes for storage. Gel electrophoresis was performed in a sodium
34
35 203 dodecyl sulfate-polyacrylamide system, and gel transfer was performed using
36
37 204 polyvinylidene fluoride membranes. The membranes were then immersed in blocking
38
39 205 buffer for 1 hour at room temperature and incubated overnight at 4°C in primary
40
41 206 antibodies against angiotensin-converting enzyme (ACE), angiotensinogen (AGT),
42
43 207 Ang II, and Ang II type 1 receptor (AT1) (Santa Cruz, USA). After washing with
44
45 208 0.1% Tris buffered saline and tween, the membranes were incubated in horseradish
46
47 209 peroxidase-conjugated secondary antibodies for 1 hour at room temperature. Protein
48
49 210 expression was observed using the ECL system (Bio-Rad, USA).
50
51
52
53
54
55
56
57
58
59
60

211 *Statistical analysis*

1
2
3
4 212 All data were processed using SPSS 19.0 (IBM, USA). Measurement data were
5
6 213 expressed as the mean \pm standard deviation (SD), t-test was used for statistical
7
8
9 214 comparisons among the data of three groups, and the Spearman correlation test was
10
11
12 215 used for correlation analysis. P values <0.05 were considered statistically significant.
13

15 216 **Result**

19 217 **General parameters of the three groups**

22
23 218 Compared with the controls, the BG level of the DM group was significantly elevated,
24
25 219 confirming that the STZ-induced diabetic model was established. Compared with the
26
27
28 220 DM group, treatment with antibiotics caused an obviously reduced BG level in the
29
30
31 221 DM+AB group (Figure 1a), suggesting that gut microbiota might be closely related to
32
33 222 the body's high BG levels under diabetic conditions. The plasma insulin level in the
34
35
36 223 three groups showed an opposite trend compared with that of BG (Figure 1b).
37
38

40 224 **Changes in gut microbiota in the three groups**

41
42
43 225 The results of 16S rDNA gene sequencing showed that there were significant
44
45 226 differences in the bacterial composition and abundance of gut microbiota between the
46
47
48 227 control and DM groups. After the application of broad-spectrum antibiotics, most of
49
50
51 228 the gut microbiota in the DM+AB group was killed (Figure 2a). The subgroup
52
53 229 sequencing analysis results of gut microbiota in each group have shown that the
54
55
56 230 abundance of *Blautia*, *Roseburia* and *Paraprevotella* in the colon of the DM group
57
58
59 231 was significantly increased compared with that of the controls (Figure 2b, 2c and 2d),
60

1
2
3
4 232 while the abundance of *Bacteroides* was relatively decreased, suggesting that the
5
6 233 composition and abundance of gut microbiota have both changed under diabetic status.
7
8
9 234 The results of the DM+AB group further confirmed the bactericidal effect of the
10
11 235 treatment of broad-spectrum antibiotics (Figure 2e).
12
13

15 236 **Treatment with antibiotics significantly reduced the level of plasma acetate**

17
18
19 237 The results of gas chromatography analysis demonstrated significantly increasing
20
21 238 plasma levels of acetate in the DM group, which might be due to the abnormalities of
22
23 239 gut microbiota under diabetic conditions. Antibiotic intervention significantly lowered
24
25 240 the plasma acetate level in the DM+AB group (Figure 3).
26
27
28
29

31 241 **The effect of gut microbiota on renal injury of incipient DN**

32
33
34 242 Compared with the controls, the ratio of kidney weight to body weight in both the DM
35
36 243 group and the DM+AB group was significantly higher (Figure 4a), indicative of renal
37
38 244 hypertrophy under the state of diabetes. In terms of proteinuria, we observed a
39
40 245 significantly increasing level of 24-hour urine protein in the DM group compared
41
42 246 with that of the control group. After the antibiotic intervention, the DM+AB group
43
44 247 had a significant reduction in 24-hour urine protein compared with that of the DM
45
46 248 group ($P<0.05$) (Figure 4b). In addition, compared with the control group, the level of
47
48 249 blood urea nitrogen (BUN) increased in both the DM group and the DM+AB group
49
50 250 ($P<0.01$), but there was no significant difference in blood creatinine among the three
51
52
53
54
55
56
57
58
59
60

1
2
3
4 251 groups (Figure 4c and 4d), suggesting that this abnormality of gut microbiota has not
5
6
7 252 yet developed to a sufficient degree to exert obvious effects on renal functions.
8
9

10 253 We next observed renal pathological changes to further evaluate the degree of renal
11
12
13 254 injury in the three groups. The results of PAS staining showed mild mesangial
14
15
16 255 expansion among the kidneys in the DM group compared with that in the DM+AB
17
18 256 group (Figure 5a-5b). Under electron microscopy, ultramicrostructural changes in the
19
20
21 257 glomerular filtration membrane in each group could be observed. The glomerular
22
23
24 258 basement membrane in the DM group was thickened, and there was fusion of
25
26 259 fenestrated endothelium, along with partly merged and missing podocyte foot
27
28
29 260 processes, which corresponds to the degree of renal injury in early DN. After the
30
31 261 antibiotic intervention, the basement membrane thickening, endothelial fusion and
32
33
34 262 podocyte injury in the DM+AB group recovered to some extent (Figure 5c). We
35
36 263 performed WGA immunofluorescence staining to observe the changes in glomerular
37
38
39 264 endothelium glycocalyx. Under laser confocal microscopy, we found that compared
40
41
42 265 with the control group, the thickness of the glomerular endothelium was significantly
43
44 266 reduced in the DM group. In the DM+AB group, the reduced glycocalyx was repaired
45
46
47 267 after the antibiotic intervention (Figure 5d). The immunofluorescence staining results
48
49
50 268 also showed significantly decreased expression of glomerular podocyte-specific
51
52 269 protein WT-1 and nephrin in the DM group compared with that in the control group,
53
54
55 270 which was relatively recovered in the DM+AB group (Figure 5e-5g), suggesting that
56
57 271 unbalanced gut microbiota might be a key factor resulting in injuries to the glomerular
58
59
60 272 filtration membrane in early DN.

273 **Intrarenal RAS is activated in early DN**

274 The measurement of circulating RAS in the three groups showed no significant
275 differences in plasma renin activity (PRA) and the level of Ang I (Figure 6a and 6b).
276 However, compared with the DM group, the concentration of Ang II in the circulation
277 was significantly reduced (Figure 6c).

278 The Western blot results to evaluate the degree of intrarenal RAS activation showed
279 that compared with the control group, the protein expression of ACE, Ang II and
280 AT1R in the kidney of the DM group was significantly increased, and antibiotic
281 treatment showed a suppressing effect on these three RAS-activating indicators
282 (Figure 6d and 6e). The expression of AGT showed an opposite trend, which might be
283 a result of negative-feedback adjustment considering its role as a rate-limiting enzyme.
284 This result suggests that the dysbiosis of the gut microbiota may be involved in the
285 intrarenal RAS activation of early DN.

286 **Correlation analysis between plasma acetate levels and intrarenal Ang II** 287 **expression**

288 To investigate the causal relationship between the dysbiosis of gut microbiota and
289 intrarenal RAS activation, we further analyzed the correlation between the plasma
290 acetate concentration and intrarenal Ang II protein expression as determined by
291 Western blot (Figure 6f). A positive correlation was observed ($r=0.969$, $P<0.001$).

292 **Discussion**

1
2
3
4 293 Most kidney diseases are characterized by an initial injury, followed by compensatory
5
6 294 growth and associated functional alterations, usually manifested as renal hypertrophy
7
8
9 295 [27]. Stages I and II of DN are mainly characterized by glomerular hypertension,
10
11 296 hyperfiltration, and renal hypertrophy [28]. Renal hypertrophy is an important and
12
13
14 297 significant marker of structural and functional changes in the kidney in early DN,
15
16
17 298 mainly characterized by glomerular cell hypertrophy, thickening of the basement
18
19 299 membrane, and an increase in the mesangial matrix. In this study, we confirmed that
20
21
22 300 the experimental animals had developed corresponding renal injury under diabetic
23
24
25 301 conditions by pathological observation.

26
27
28 302 The RAS can be divided into the circulatory and local RAS depending on its location
29
30
31 303 of synthesis and action. In circulating RAS, Ang II is produced under the serial effects
32
33
34 304 of renin secreted by the kidney, angiotensin from the liver, and ACE located in
35
36 305 vascular endothelial cells. In certain organs or cells, the synthesis of RAS components
37
38
39 306 is independent. Ang II can be produced in the intercellular space [29] under the effect
40
41
42 307 of enzymes other than renin and ACE (such as chymase) and exerts many
43
44 308 pathophysiological effects by activating AT1R [30]. The activation of RAS has
45
46
47 309 always been considered an important factor in the development of DN, and local RAS
48
49
50 310 seems to be more involved compared with the circulating RAS [31]. The kidney itself
51
52 311 contains all the RAS components [32]. High glucose has been reported to promote the
53
54
55 312 production of Ang II, which in turn leads to glomerular hyperfiltration and high
56
57 313 permeability, as well as extracellular matrix deposition [33]. Clinical application of
58
59
60 314 RAS inhibitors could significantly retard the development of proteinuria in DN

1
2
3
4 315 patients and lower the incidence of ESRD. As a current first-line treatment for DN,
5
6 316 the efficacy of RAS inhibitors in preventing DN is still very limited. The rising
7
8
9 317 prevalence of DN has suggested that a deeper understanding of the molecular
10
11 318 mechanisms underlying DN is required to seek better treatment.

12
13
14
15 319 The relationship between gut microbiota and many metabolic diseases has been a
16
17 320 hotpot for research in recent years. Under normal circumstances, *Firmicutes* and
18
19 321 *Bacteroidetes* take up a large proportion of the whole microbiota in the gut, while the
20
21 322 composition of other phyla varies individually due to several factors, such as genetics,
22
23 323 diet and antibiotic use. However, under pathological conditions, the species and
24
25 324 abundance of the host gut microbiota would change significantly, mainly
26
27 325 characterized by decreasing normally dominant bacteria and increasing pathogenic
28
29 326 bacteria. It has also been shown in this study that compared to the control group, there
30
31 327 was microecological dysbiosis of gut microbiota in the intestinal tract of diabetic rats.
32
33 328 The application of antibiotic intervention is a common method used in studies of gut
34
35 329 microbiota and its role in the development of diseases. In this study, we observed that
36
37 330 the intervention of antibiotics affected many aspects of the DN animal model, from
38
39 331 basic functions and pathological changes in the kidneys to the amount of products
40
41 332 released from gut microbiota. The use of mixed antibiotics has ensured the killing
42
43 333 effect of the bacteria in the intestinal tract of experimental animals, and in the
44
45 334 meantime, it could also attenuate the renal injury of early DN, including reducing the
46
47 335 amount of 24-hour urine protein and mitigating the injury to the glomerular filtration
48
49 336 membrane and the pathological changes in the tubules.
50
51
52
53
54
55
56
57
58
59
60

1
2
3
4 337 SCFAs are a major product of the fermentation of carbohydrates by gut microbiota,
5
6 338 and there are three main types: acetate, propionate, and butyrate. The
7
8
9 339 butyrate-producing microbiota is essential in maintaining the balance of the intestinal
10
11 340 environment in humans. However, the number of butyrate-producing microbiota in
12
13 341 diabetic patients is significantly reduced, while the number of other opportunistic
14
15 342 pathogens shows an increasing trend. There is evidence that a butyrate-producing
16
17 343 *Clostridium* genus could exert antidiabetic effects by increasing the production of
18
19 344 butyrate and upregulating the expression of SCFA receptors in the gut [34]. As a main
20
21 345 SCFA product of gut microbiota, acetate has demonstrated an intricate effect on the
22
23 346 internal environment. It has been reported that acetate is almost undetectable in the
24
25 347 blood of germ-free mice [23], while the content of acetate in animals with a high-fat
26
27 348 diet is significantly increased, indicating that the level of acetate might be a potential
28
29 349 indicator of the activity of gut microbiota. This study has shown that antibiotic
30
31 350 intervention significantly reduced the relatively higher plasma level of acetate in
32
33 351 diabetic rats, considering the alleviated renal lesions after antibiotic intervention. It
34
35 352 can be speculated that overproduction of acetate might be adverse to the development
36
37 353 of early DN. However, the causal relationship between gut microbiota dysbiosis and
38
39 354 the development of DN remains to be elucidated, and more explorations may provide
40
41 355 a new perspective and therapeutic target for the future diagnosis and treatment of DN.
42
43
44
45
46
47
48
49
50
51
52
53
54 356 RAS activation has been considered one of the important initiating factors in the early
55
56 357 development of DN, yet the exact associations between gut microbiota and RAS
57
58 358 activation remain to be elucidated. Pluznick J *et al* [24] found that signals from the

1
2
3
4 359 gut microbiota, i.e., SCFAs, could be received by corresponding receptors expressed
5
6 360 at renal small arterioles, further regulating the secretion of renin, which was involved
7
8
9 361 in maintaining glomerular pressure. This process could be blocked by antibiotics or
10
11 362 knockout of the SCFA receptor. Considering the characteristics of glomerular
12
13 363 hypertension and hyperfiltration in the early stage of DN, the disordered gut
14
15 364 microbiota is likely to generate excessive SCFAs, which bind to corresponding
16
17 365 receptors in the kidney and regulate RAS, thus promoting the pathological changes in
18
19
20 366 early DN. In this study, we have shown that in the early stage of DN, the expression
21
22
23 367 of RAS in the kidney was significantly elevated, indicating RAS activation at this
24
25
26 368 stage. After antibiotic intervention, the level of circulating Ang II was lowered, and
27
28
29 369 the expression of RAS within the kidney was also significantly weakened, suggesting
30
31
32 370 that there might be a causal relationship between the dysbiosis of gut microbiota and
33
34
35 371 intrarenal RAS activation in early DN. Therapeutic intervention could be applied to
36
37
38 372 change the composition of gut microbiota, focusing on the preservation of beneficial
39
40
41 373 phyla, to create renoprotective prospects [35].

42
43
44 374 In summary, we have established a DN model to observe the changes in gut
45
46
47 375 microbiota and its metabolite acetate in early DN and to further investigate the
48
49
50 376 association between these changes and RAS activation in the kidney to elucidate the
51
52
53 377 underlying mechanism of early renal injury in DN. Further exploration of the causal
54
55
56 378 relationship and intricate mechanism of gut microbiota and RAS activation in the
57
58
59 379 early development of DN are required to develop new prevention strategies for
60 380 clinical early DN.

1
2
3
4 **381 Acknowledgments**
5
6
7

8 **382** This work was supported by the National Natural Science Foundation of China (grant
9
10 **383** 81970629), the Jiangsu Province Social Development Project (BE2018744), the
11
12 **384** Project for Jiangsu Provincial Medical Talent (ZDRCA2016077), the Jiangsu
13
14 **385** Province Six Talent Peaks Project (2015-WSN-002), the Fundamental Research
15
16 **386** Funds for the Central Universities (KYCX18-0182, KYCX17-0169, KYZZ15-0061),
17
18 **387** the Jiangsu Province Ordinary University Graduate Research Innovation Project
19
20 **388** (SJZZ16-004), and the Joint Project of Southeast University and Pharmaceutical
21
22 **389** University of China (2242019K3DZ03).
23
24
25
26
27
28
29

30 **390 Author contribution**
31
32

33 **391** Chen Chen Lu performed the research, analyzed the data and wrote the manuscript;
34
35 **392** Kun Ling Ma designed and reviewed the manuscript; Ze Bo Hu, Ru Wang, Ze Hui
36
37 **393** Hong, Jian Lu, Pei Pei Chen, Jia Xiu Zhang, Xue Qi Li, Ben Yin Yuan, and Si Jia
38
39 **394** Huang assisted in the research; Xiong-zhong Ruan and Bi-cheng Liu analyzed and
40
41 **395** interpreted the data. All authors read and approved the final manuscript.
42
43
44
45
46
47
48
49
50
51
52
53
54
55
56
57
58
59
60

397 **References**

- 398 1. Cho NH, Shaw JE, Karuranga S, Huang Y, da Rocha Fernandes JD, Ohlrogge
399 AW, et al. IDF Diabetes Atlas: Global estimates of diabetes prevalence for
400 2017 and projections for 2045. *Diabetes Res Clin Pract.* 2018;138:271-281.
- 401 2. Xu Y, Wang L, He J, Bi Y, Li M, Wang T, et al. Prevalence and control of
402 diabetes in Chinese adults. *JAMA.* 2013;310:948-59.
- 403 3. Tamura J, Konno A, Hashimoto Y, Kon Y. Upregulation of renal
404 renin-angiotensin system in mouse diabetic nephropathy. *Jpn J Vet Res.*
405 2005;53:13-26.
- 406 4. Kanasaki K, Taduri G, Koya D. Diabetic nephropathy: the role of
407 inflammation in fibroblast activation and kidney fibrosis. *Front Endocrinol*
408 (Lausanne). 2013;4:7.
- 409 5. Pichler R, Afkarian M, Dieter BP, Tuttle KR. Immunity and inflammation in
410 diabetic kidney disease: translating mechanisms to biomarkers and treatment
411 targets. *Am J Physiol Renal Physiol.* 2017;312:716-31.
- 412 6. Miranda-Diaz AG, Pazarin-Villasenor L, Yanowsky-Escatell FG,
413 Andrade-Sierra J. Oxidative Stress in Diabetic Nephropathy with Early
414 Chronic Kidney Disease. *J Diabetes Res.* 2016;2016:7047238.
- 415 7. Urushihara M, Kagami S. Role of the intrarenal renin-angiotensin system in
416 the progression of renal disease. *Pediatr Nephrol.* 2017;32:1471-79.
- 417 8. Schroeder BO, Backhed F. Signals from the gut microbiota to distant organs in
418 physiology and disease. *Nat Med.* 2016;22:1079-89.

- 1
2
3
4 419 9. Org E, Mehrabian M, Lusic AJ. Unraveling the environmental and genetic
5
6 420 interactions in atherosclerosis: Central role of the gut microbiota.
7
8
9 421 *Atherosclerosis*. 2015;241:387-99.
- 10
11 422 10. Tilg H, Moschen AR. Microbiota and diabetes: an evolving relationship. *Gut*.
12
13 423 2014;63:1513-21.
- 14
15
16 424 11. Qin J, Li Y, Cai Z, Li S, Zhu J, Zhang F, et al. A metagenome-wide
17
18 425 association study of gut microbiota in type 2 diabetes. *Nature*.
19
20 426 2012;490:55-60.
- 21
22
23 427 12. Karlsson FH, Tremaroli V, Nookaew I, Bergstrom G, Behre CJ, Fagerberg B,
24
25 428 et al. Gut metagenome in European women with normal, impaired and
26
27 429 diabetic glucose control. *Nature*. 2013;498:99-103.
- 28
29
30 430 13. Louis P, Young P, Holtrop G, Flint HJ. Diversity of human colonic
31
32 431 butyrate-producing bacteria revealed by analysis of the butyryl-CoA:acetate
33
34 432 CoA-transferase gene. *Environ Microbiol*. 2010;12:304-14.
- 35
36
37 433 14. Furet JP, Kong LC, Tap J, Poitou C, Basdevant A, Bouillot JL, et al.
38
39 434 Differential adaptation of human gut microbiota to bariatric surgery-induced
40
41 435 weight loss: links with metabolic and low-grade inflammation markers.
42
43 436 *Diabetes*. 2010;59:3049-57.
- 44
45
46 437 15. Vrieze A, Van Nood E, Holleman F, Salojarvi J, Kootte RS, Bartelsman JF, et
47
48 438 al. Transfer of intestinal microbiota from lean donors increases insulin
49
50 439 sensitivity in individuals with metabolic syndrome. *Gastroenterology*.
51
52 440 2012;143:913-6.
- 53
54
55
56
57
58
59
60

- 1
2
3
4 441 16. Larsen N, Vogensen FK, van den Berg FW, Nielsen DS, Andreasen AS,
5
6 442 Pedersen BK, et al. Gut microbiota in human adults with type 2 diabetes
7
8
9 443 differs from non-diabetic adults. *PLoS One*. 2010;5:e9085.
10
11 444 17. Murri M, Leiva I, Gomez-Zumaquero JM, Tinahones FJ, Cardona F, Soriguer
12
13 F, et al. Gut microbiota in children with type 1 diabetes differs from that in
14 445
15 healthy children: a case-control study. *BMC Med*. 2013;11:46.
16 446
17
18 447 18. Giongo A, Gano KA, Crabb DB, Mukherjee N, Novelo LL, Casella G, et al.
19
20 448 Toward defining the autoimmune microbiome for type 1 diabetes. *ISME J*.
21
22 449 2011;5:82-91.
23
24
25 450 19. Cani PD, Neyrinck AM, Fava F, Knauf C, Burcelin RG, Tuohy KM, et al.
26
27 451 Selective increases of bifidobacteria in gut microflora improve
28
29 452 high-fat-diet-induced diabetes in mice through a mechanism associated with
30
31 endotoxaemia. *Diabetologia*. 2007;50:2374-83.
32 453
33
34 454 20. Stilling RM, van de Wouw M, Clarke G, Stanton C, Dinan TG, Cryan JF. The
35
36 455 neuropharmacology of butyrate: The bread and butter of the
37
38 456 microbiota-gut-brain axis? *Neurochem Int*. 2016;99:110-132.
39
40
41 457 21. Vinolo MA, Rodrigues HG, Nachbar RT, Curi R. Regulation of inflammation
42
43 458 by short chain fatty acids. *Nutrients*. 2011;3:858-76.
44
45
46 459 22. Kim MH, Kang SG, Park JH, Yanagisawa M, Kim CH. Short-chain fatty acids
47
48 460 activate GPR41 and GPR43 on intestinal epithelial cells to promote
49
50 461 inflammatory responses in mice. *Gastroenterology*. 2013;145:396-406.
51
52
53 462 23. Perry RJ, Peng L, Barry NA, Cline GW, Zhang D, Cardone RL, et al. Acetate
54
55
56
57
58
59
60

- 1
2
3
4 463 mediates a microbiome-brain-beta-cell axis to promote metabolic syndrome.
5
6 464 Nature. 2016;534:213-7.
7
8
9 465 24. Pluznick J, Protzko R, Gevorgyan H, Peterlin Z, Sipos A, Han J, et al.
10
11 466 Olfactory receptor responding to gut microbiota-derived signals plays a role in
12
13 467 renin secretion and blood pressure regulation. Proc Natl Acad Sci U S A.
14
15 468 2013;110:4410-5.
16
17
18 469 25. Brown D, Sorscher EJ, Ausiello DA, Benos DJ. Immunocytochemical
19
20 470 localization of Na⁺ channels in rat kidney medulla. Am J Physiol.
21
22 471 1989;256:366-9.
23
24
25 472 26. Kantorowicz L, Valego NK, Tang L, Figueroa JP, Chappell MC, Carey LC, et
26
27 473 al. Plasma and renal renin concentrations in adult sheep after prenatal
28
29 474 betamethasone exposure. Reprod Sci. 2008;15:831-8.
30
31
32 475 27. Hostetter TH. Progression of renal disease and renal hypertrophy. Annu Rev
33
34 476 Physiol. 1995;57:263-78.
35
36
37 477 28. Mogensen CE, Christensen CK, Vittinghus E. The stages in diabetic renal
38
39 478 disease. With emphasis on the stage of incipient diabetic nephropathy.
40
41 479 Diabetes. 1983;32 Suppl 2:64-78.
42
43
44 480 29. Kumar R, Thomas CM, Yong QC, Chen W, Baker KM. The intracrine
45
46 481 renin-angiotensin system. Clin Sci (Lond). 2012;123:273-84.
47
48
49 482 30. Hunyady L, Catt KJ. Pleiotropic AT1 receptor signaling pathways mediating
50
51 483 physiological and pathogenic actions of angiotensin II. Mol Endocrinol.
52
53 484 2006;20:953-70.
54
55
56
57
58
59
60

- 1
2
3
4 485 31. Wysocki J, Ye M, Khattab AM, Fogo A, Martin A, David NV, et al.
5
6 486 Angiotensin-converting enzyme 2 amplification limited to the circulation does
7
8 487 not protect mice from development of diabetic nephropathy. *Kidney Int.*
9
10 488 2017;91:1336-1346.
11
12
13
14 489 32. Navar LG, Inscho EW, Majid SA, Imig JD, Harrison-Bernard LM, Mitchell
15
16 490 KD. Paracrine regulation of the renal microcirculation. *Physiol Rev.*
17
18 491 1996;76:425-536.
19
20
21
22 492 33. Carey RM, Siragy HM. The intrarenal renin-angiotensin system and diabetic
23
24 493 nephropathy. *Trends Endocrinol Metab.* 2003;14:274-81.
25
26
27 494 34. Jia L, Li D, Feng N, Shamon M, Sun Z, Ding L, et al. Anti-diabetic Effects
28
29 495 of *Clostridium butyricum* CGMCC0313.1 through Promoting the Growth of
30
31 496 Gut Butyrate-producing Bacteria in Type 2 Diabetic Mice. *Sci Rep.*
32
33 497 2017;7:7046.
34
35
36
37 498 35. Tang WH, Kitai T, Hazen SL. Gut Microbiota in Cardiovascular Health and
38
39 499 Disease. *Circ Res.* 2017;120:1183-1196.
40
41
42

43 500
44
45
46
47
48
49
50
51
52
53
54
55
56
57
58
59
60

1
2
3 502 **Figure legends**
4
5

6 503 **Figure 1. General parameters of the three groups**
7
8
9

10 504 (a) Blood glucose levels. (b) Plasma insulin levels. * $P < 0.01$ compared with the
11
12 505 control group, # $P < 0.05$ compared with the DM group.
13
14

15
16 506 **Figure 2. The changes in gut microbiota in the three groups**
17
18

19 507 (a) Taxonomic cladogram derived from LEfSe analysis of 16S sequences. Red shaded
20
21 508 areas indicate control-enriched taxa, green shaded areas indicate DM-enriched taxa,
22
23 509 and blue shaded areas indicate DM+AB-enriched taxa. (b-e) Subgroup sequencing
24
25 510 analysis of gut microbiota. Class A indicates the control group, Class B indicates the
26
27 511 DM group, and Class C indicates the DM+AB group. The solid and dashed lines
28
29 512 indicate the average and median relative abundance, respectively. (b) The relative
30
31 513 abundance of *Blautia* in the gut microbiota of the three groups. (c) The relative
32
33 514 abundance of *Roseburia* in the gut microbiota of the three groups. (d) The relative
34
35 515 abundance of *Paraprevotella* in the gut microbiota of the three groups. (e) The relative
36
37 516 abundance of *Bacteroides* in the gut microbiota of the three groups.
38
39
40
41
42
43
44
45
46
47
48
49
50
51
52
53
54
55
56
57
58
59
60

1
2
3 518 **Figure 3. Treatment with antibiotics significantly reduced the level of plasma**
4
5 519 **acetate**
6
7

8
9 520 Plasma level of acetate. * $P < 0.01$ compared with the control group, # $P < 0.05$ compared
10
11 521 with the DM group.
12

13
14
15 522 **Figure 4. The effect of gut microbiota on renal indicators of incipient DN**
16

17
18 523 (a) Kidney weight-to-body weight ratios. (b) 24-hour urine protein. (c) Blood urea
19
20 524 nitrogen (BUN) level. (d) Blood creatinine. * $P < 0.01$ compared with the control group,
21
22 525 # $P < 0.05$ compared with the DM group.
23
24

25
26 526 **Figure 5. The effect of gut microbiota on renal injuries of incipient DN**
27

28
29
30 527 (a) Pathological changes were assessed by PAS staining (original magnification,
31
32 528 $\times 400$). (b) The score of mesangial expansion was determined from histology sections.
33
34 529 *** $P < 0.01$ compared with the control, # $P < 0.05$ compared with the DM group. (c)
35
36 530 Changes in podocytes were evaluated by electron microscopy (original magnification,
37
38 531 $\times 12000$). (d) The changes in glomerular endothelium glycocalyx were assessed by
39
40 532 WGA staining (original magnification, $\times 400$). (e) WT-1 and nephrin protein
41
42 533 expression was evaluated by immunofluorescent staining (original magnification,
43
44 534 $\times 400$). The arrows indicate glomerular endothelium glycocalyx. (f) Quantitation of
45
46 535 immunofluorescence staining for WT-1. * $P < 0.05$; compared with the control;
47
48 536 ## $P < 0.01$ compared with DM. (g) Quantitation of immunofluorescence staining for
49
50 537 nephrin. *** $P < 0.001$; compared with the control; # $P < 0.05$ compared with DM.
51
52
53
54
55
56
57
58
59
60

1
2
3 **539 Figure 6. Intrarenal RAS is activated in early DN**
4

5
6
7 540 Plasma renin activity level (a), Ang I level (b) and Ang II level (c). The protein
8
9 541 expression levels of RAS were measured by Western blotting (d). The histograms
10
11 542 represent the mean±SD of the densitometric scans of the protein bands normalized to
12
13 543 β-actin (e). Correlation analysis of plasma acetate levels and intrarenal Ang II
14
15 544 expression levels (f) ($r=0.969$, $P<0.001$). * $P<0.01$ compared with the control group,
16
17
18 545 # $P<0.05$ compared with the DM group.
19
20
21
22
23
24
25
26
27
28
29
30
31
32
33
34
35
36
37
38
39
40
41
42
43
44
45
46
47
48
49
50
51
52
53
54
55
56
57
58
59
60

Figures

Figure. 1

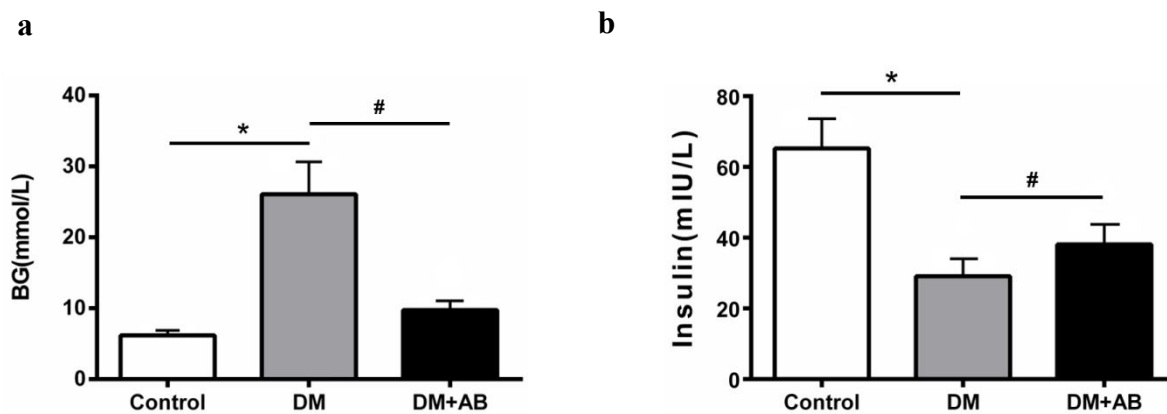
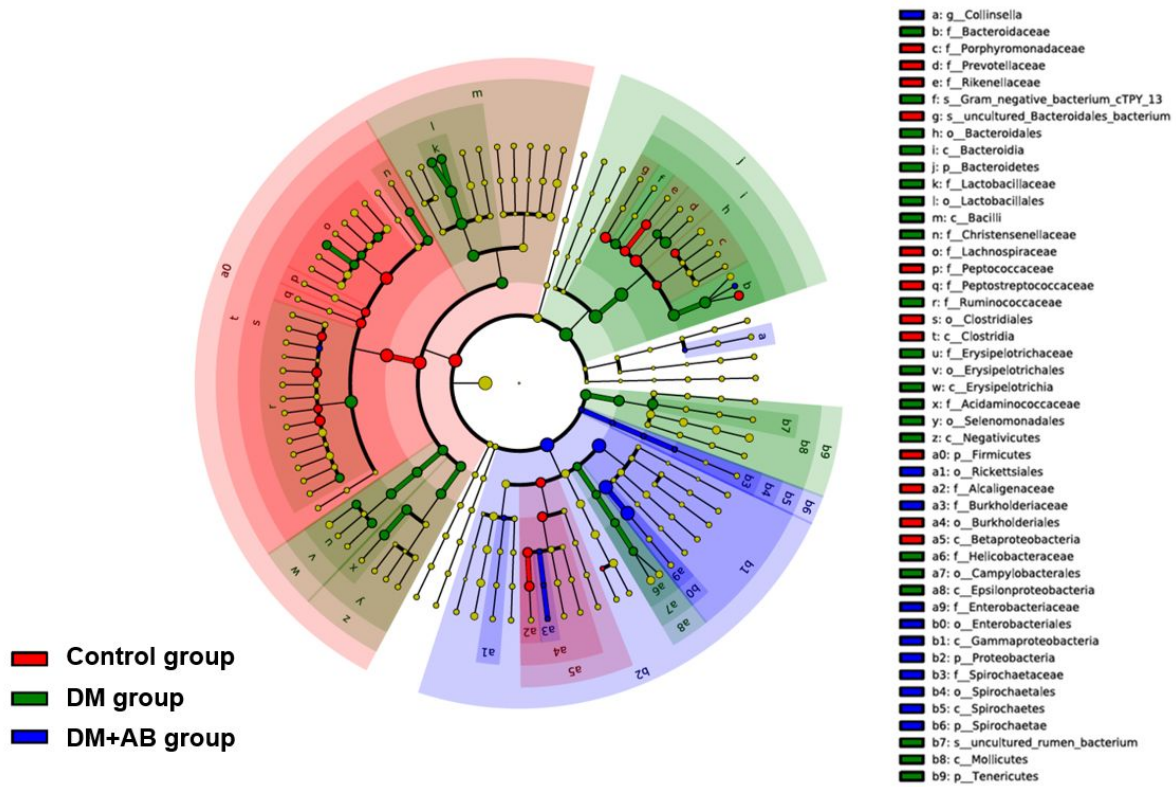
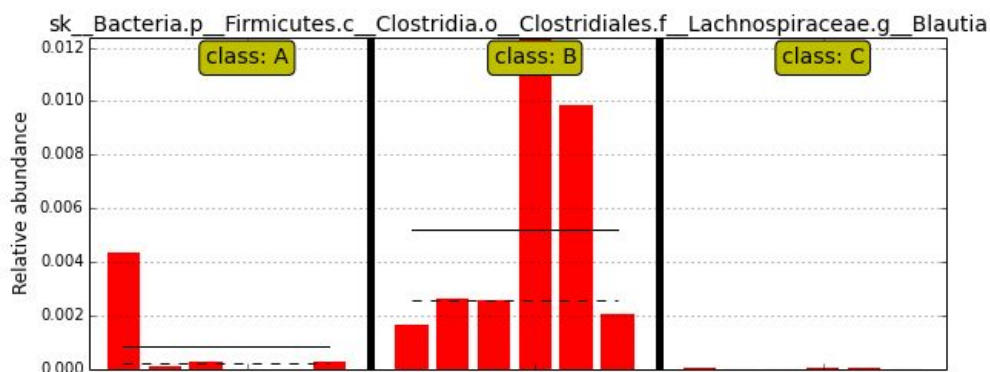


Figure. 2

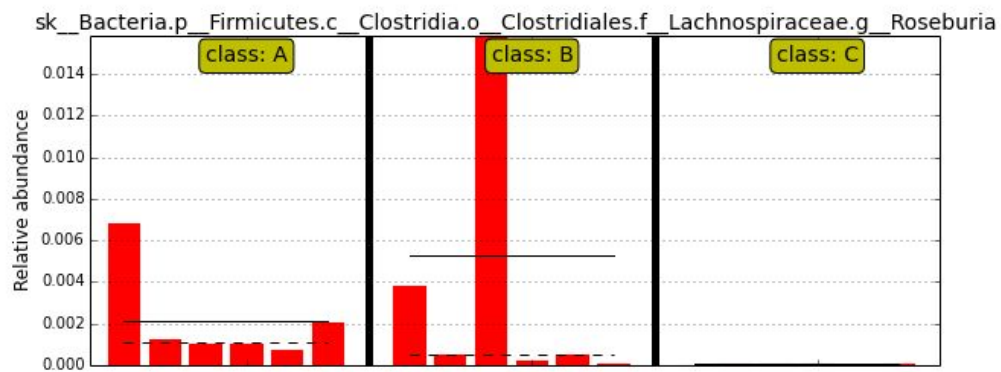
a



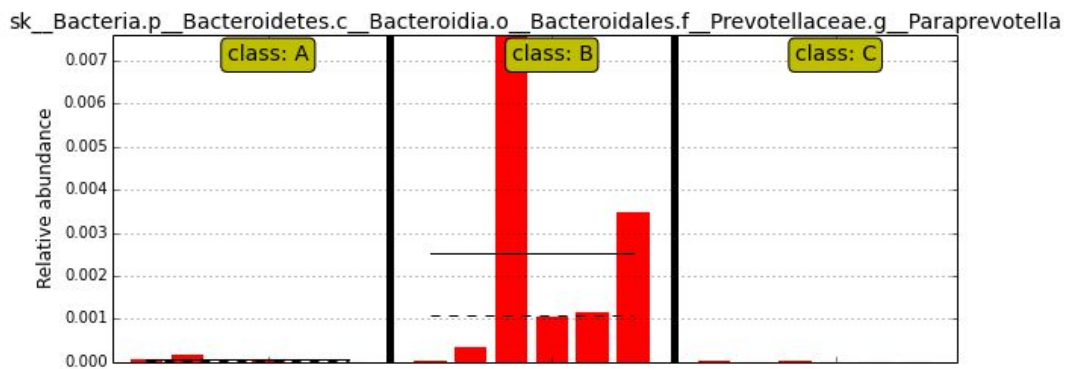
b



c



d



e

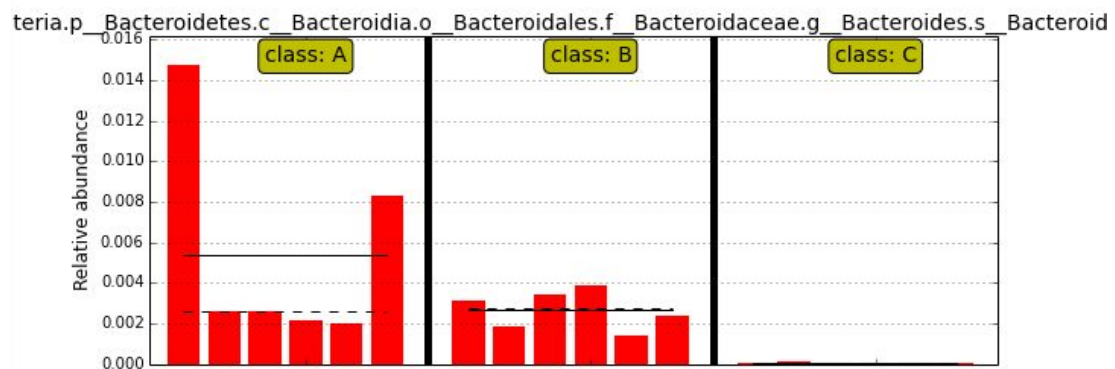


Figure.3

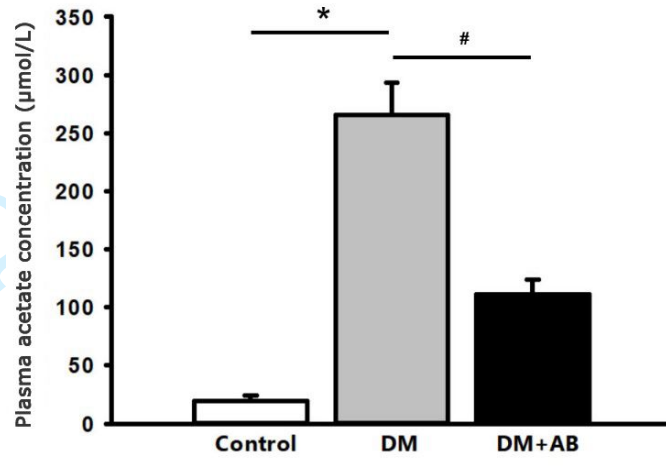


Figure. 4

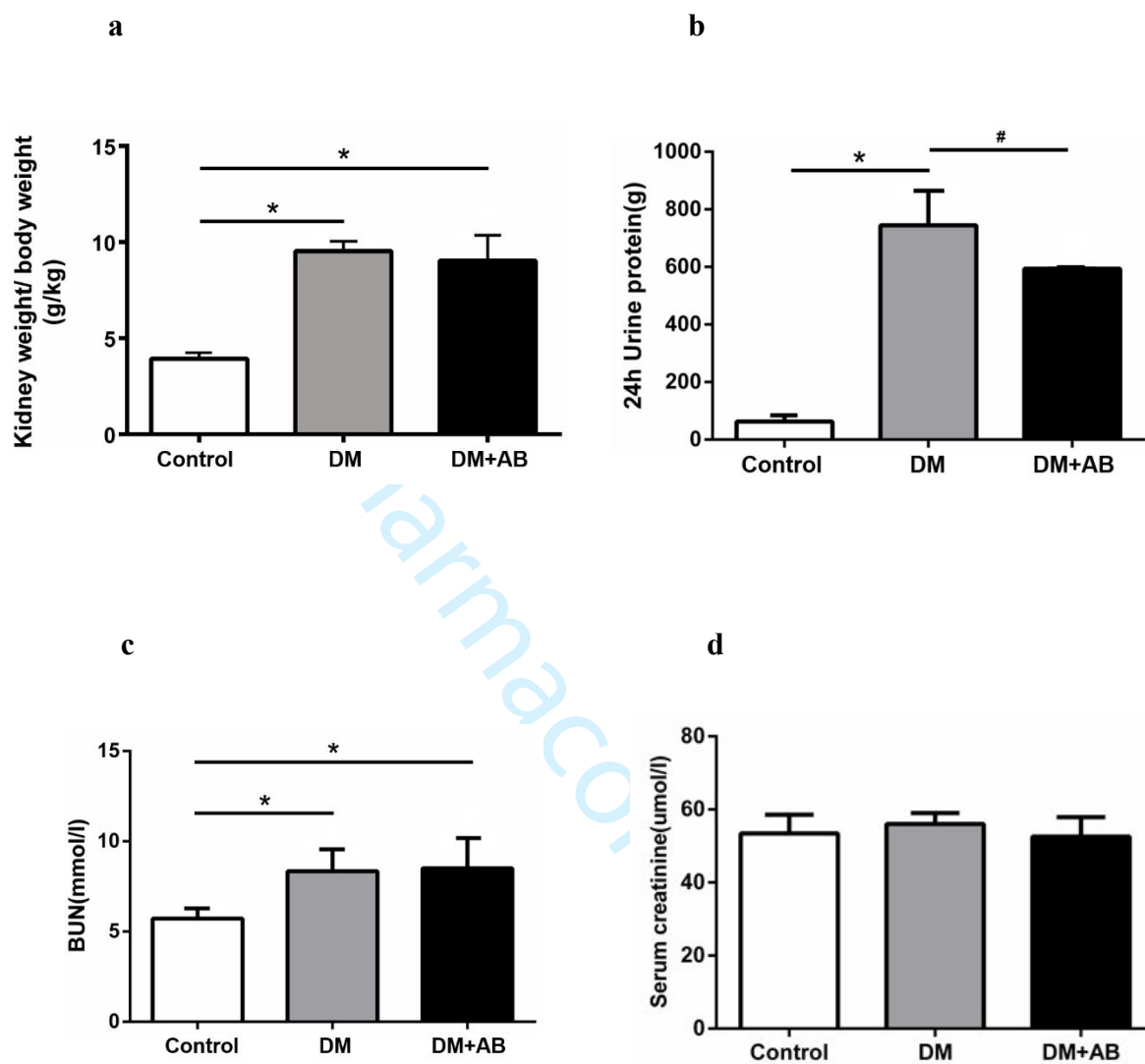
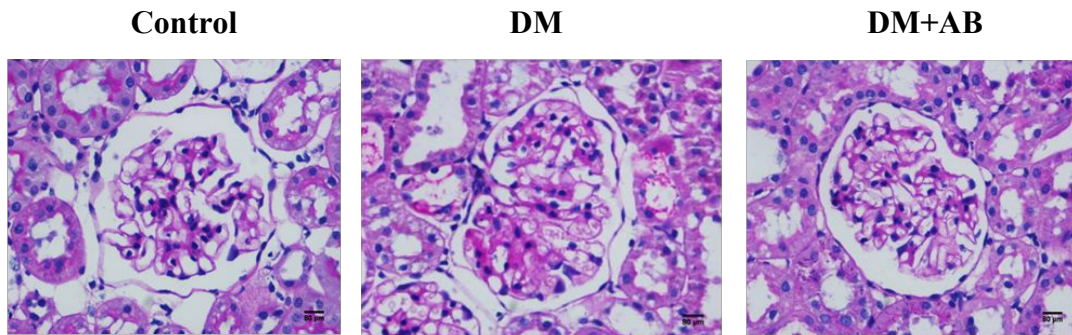
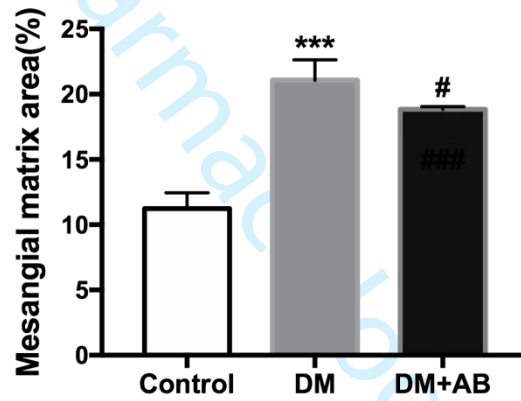


Figure. 5

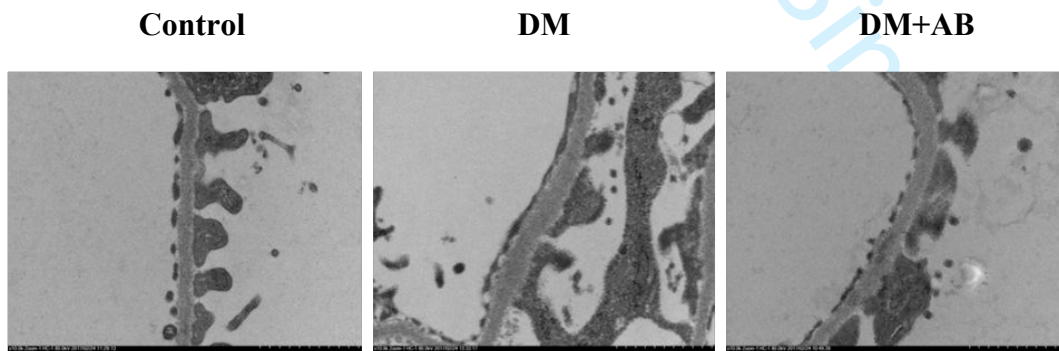
a



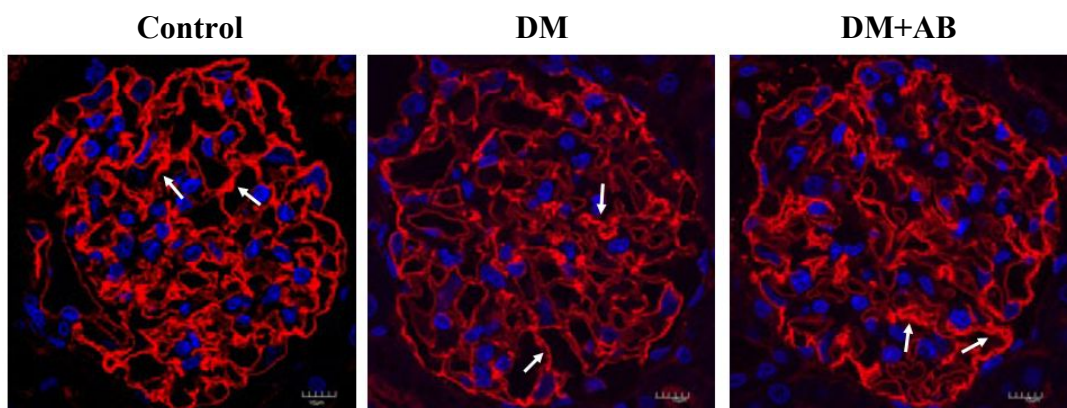
b



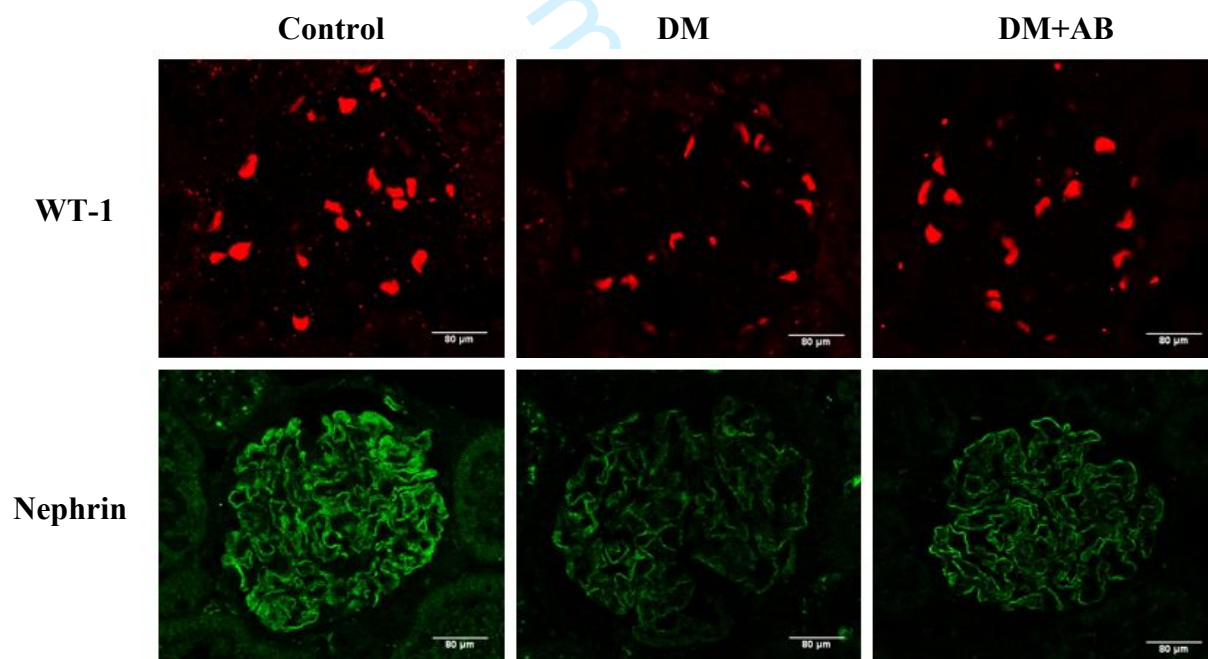
c



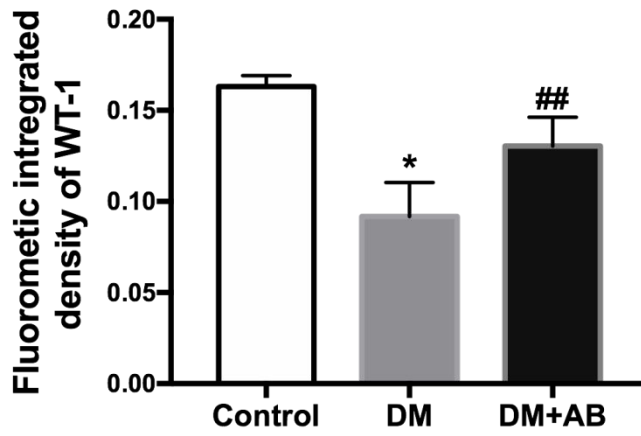
d



e



f



g

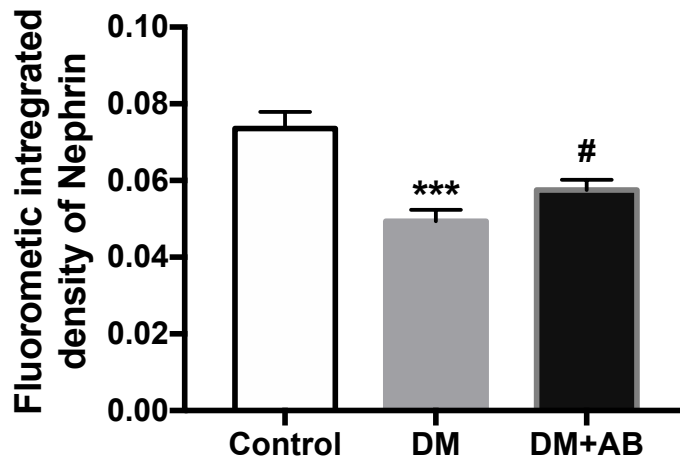
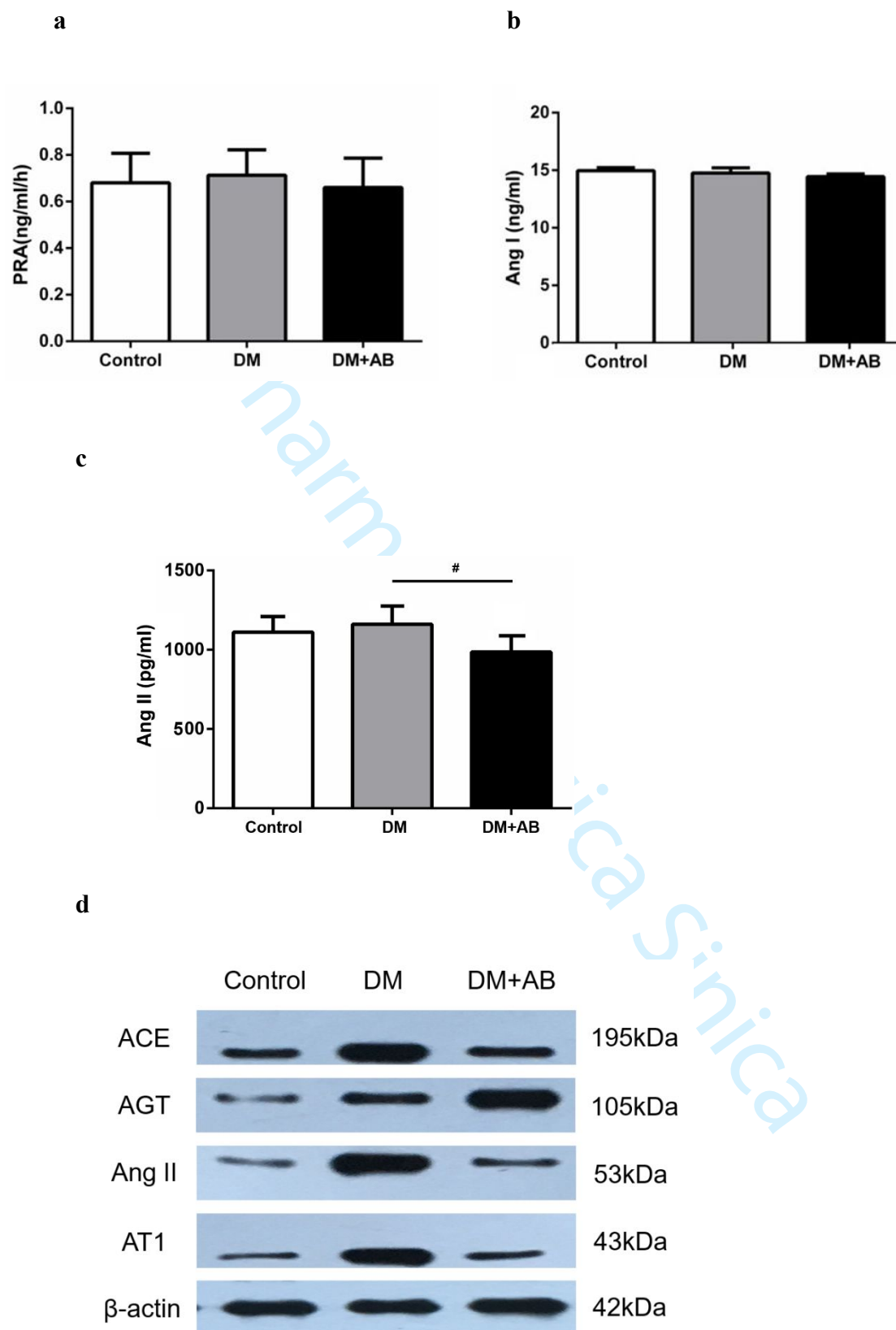
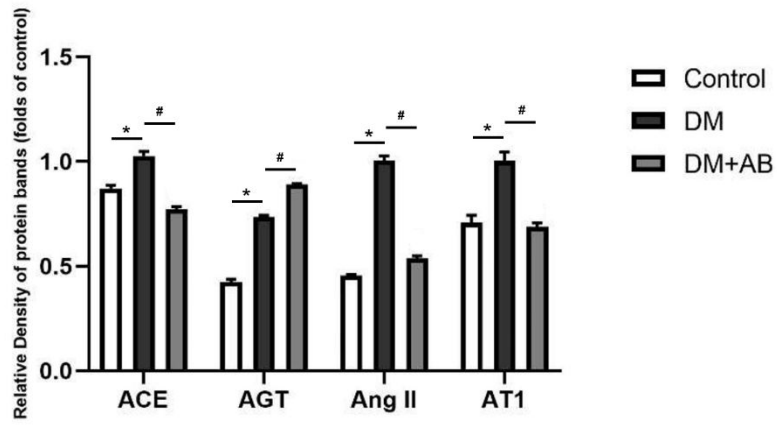


Figure. 6



e



f

